

# Performance Enhancement of 2-D OCDMA Systems Using Multi-Code Modulation and Heterodyne Detection

Ngoc T. Dang, *Student Member, IEEE* and Anh T. Pham, *Member, IEEE*

Computer Communications Lab., The University of Aizu, Tsugura, Ikki-machi, Aizuwakamatsu, 965-8580, Japan  
Tel: (+81) 242 37 2791, Fax: (+81) 242 37 2750, e-mail: pham@u-aizu.ac.jp

## ABSTRACT

A new modulation scheme for 2-D OCDMA systems named multi-code modulation (MCM) is proposed in this paper. The key advantage of MCM over the conventional ones is the ability of mitigating simultaneously both multiple access interference and dispersion. We also propose to combine MCM with heterodyne detection, a powerful technique to relax optical beating interference, to obtain better performance. The numerical results show that the proposed system allows for lower bit error rate, lower required power, and higher user's bit rate than that of conventional ones using other modulation schemes such as on-off keying modulation, pulse amplitude modulation, and pulse position modulation.

**Keywords:** two-dimensional OCDMA, multi-code modulation, pulse position modulation, heterodyne detection.

## 1. INTRODUCTION

Optical code-division multiple-access (OCDMA) has received increasing interest as a promising technique for next generation broadband access networks. Early works focused on one-dimensional (1-D) OCDMA systems, which use only time domain for encoding. To achieve better system performance in term of both bit-error rate (BER) and number of supportable users, 2-D OCDMA systems in which transmitted signal is encoded using both time and frequency domains have been proposed and received more interest [1].

The feasibility of 2-D OCDMA systems in broadband access networks is primarily influenced by physical layer impairments. These impairments include various noises, interferences, and dispersions. Especially, multiple access interference (MAI), optical beating interference (OBI), and group velocity dispersion (GVD) are the main factors that degrade the system performance [2-5]. MAI and OBI limit the number of supportable users whereas GVD limits the transmission length and/or increases the required power of the system.

Several methods have been proposed to mitigate the impact of MAI, OBI, and GVD. To reduce MAI, pulse position modulation (PPM) is recommended as an efficient method. The use of PPM becomes even more effective when it is combined with heterodyne detection, the powerful receiver structure that helps to relax OBI [3]. However, both PPM and heterodyne detection cannot lessen the impact of GVD, which becomes even stronger in PPM systems due to the narrowing of pulse width. On the contrary, pulse amplitude modulation (PAM) can be utilized to increase the pulse width hence reduce the impact of GVD. However, the performance of OCDMA systems using PAM is significantly deteriorated due to MAI pulses with high intensities even when the number of MAI pulses is small [4].

We therefore propose a new modulation scheme called multi-code modulation (MCM), which can solve all of above-mentioned issues. In MCM, each block of  $m$ -bit is also mapped into  $M$  symbols. However, instead of using position or amplitude for encoding, each symbol is encoded by a corresponding code, which helps to decrease the impact of both GVD and MAI. To detect symbols, maximum likelihood detection is employed like in PPM. As a result, MCM has abilities of simultaneously mitigating both GVD and MAI, which are inherited from PAM and PPM, respectively. We also propose to combine MCM with heterodyne detection to relax the impact of OBI thus obtain better performance.

## 2. CONSTRUCTION OF MULTI-CODE SYMBOLS

### 2.1 2-D Prime Code

A code used in 2-D OCDMA systems is the combination of a time-spreading (TS) pattern and a wavelength-hopping (WH) pattern. In this paper, we use prime code for both patterns. A TS pattern can be generated using the linear congruent placement operator, to place a pulse within a block as  $a_{xy} = [x, y]$  where  $x, y = 0, 1, \dots, p_s - 1$ ,  $p_s$  is a prime number, and  $[\cdot]$  denotes modulo  $p_s$  operation [1]. The algorithm determines the place of a pulse within a block of length  $p_s$ . A code pattern consisting of  $p_s$  such blocks. Similarly, a WH pattern is generated from a prime number  $p_h$  ( $p_s \leq p_h$ ). The process of generating the TS and the WH patterns is illustrated in Table 1.

The WH pattern  $H_0$  comprises pulses at one wavelength only, as evident from Table 1, and is therefore discarded. Hence the number of WH patterns is  $p_h - 1$ , the number of TS patterns being  $p_s$ . Thus a 2-D code set, including  $p_s(p_h - 1)$  distinctive 2-D prime codes of length  $p_s^2$ , can be generated. The code weight is  $p_s$  and the maximum cross-correlation between two 2-D prime codes is one [1].

### 2.2 Construction of Multi-code Symbols

Each user is assigned  $M$  2-D prime codes to encode its  $M$  symbols. These  $M$  2-D codes can be a part of one single code set of  $(p_s, p_h)$  or  $M$  different code sets of  $(p_s, p_h^*)$  as follows.

**Using a single code set:** We equally divide  $p_s(p_h - 1)$  codes of a code set to all users,  $M$  codes to each user. The maximum number of users in this case is  $\lfloor p_s(p_h - 1)/M \rfloor$ , where  $\lfloor x \rfloor$  defines floor function of  $x$ .

**Using multiple code sets:** For each user,  $M$  codes are generated from one TS pattern in combination with  $M$  WH patterns which belong to  $M$  different wavelength groups. Each group includes  $p_h^*$  wavelengths with the condition that  $p_h^*$  is also a prime number and  $p_s \leq p_h^*$ . There are total  $M$  code sets of  $(p_s, p_h^*)$ , each one is used to encode the same symbol of all users. An example of MC symbols is illustrated in Table 2. In this table,  $H_{uv}$  is denoted for the  $v$ -th WH pattern ( $v = 1, \dots, p_h^* - 1$ ) of the  $u$ -th wavelength group ( $u = 0, \dots, M - 1$ ). In this case, the system totally use 6 (i.e.,  $Mp_h^*$ ) wavelengths and can support maximum 6 (i.e.,  $p_s(p_h^* - 1)$ ) users with  $M = 2$ .

Table 1. WH and TS patterns for  $p_s = p_h = 3$ .

WH pattern	TS pattern
$H_0 \quad \lambda_0 \lambda_0 \lambda_0$	$S_0 \quad 100 \quad 100 \quad 100$
$H_1 \quad \lambda_0 \lambda_1 \lambda_2$	$S_1 \quad 100 \quad 010 \quad 001$
$H_2 \quad \lambda_0 \lambda_2 \lambda_1$	$S_2 \quad 100 \quad 001 \quad 010$

Table 2. Multiple code sets:  $p_s = p_h^* = 3$  and  $M = 2$ .

TS	WH of group 0 ( $s_0$ )	WH of group 1 ( $s_1$ )	User
$S_z$	$H_{01}$	$H_{11}$	User $_{z1}$
	$H_{02}$	$H_{12}$	User $_{z2}$
$z = 0, 1, 2$			

### 3. SYSTEM DESCRIPTIONS

A schematic diagram of a 2-D OCDMA system using MCM and heterodyne detection is shown in Fig. 1. For illustrative purposes, one transmitter and one receiver are depicted in detail in the figure.

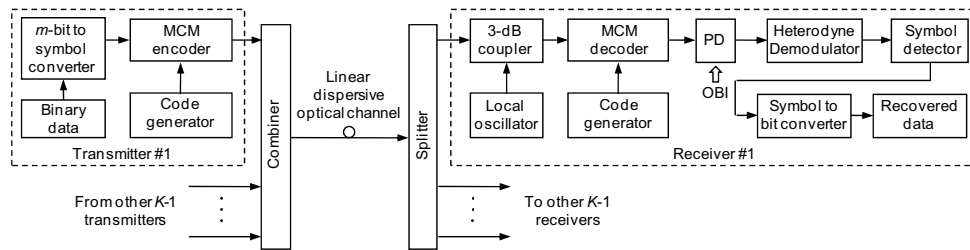


Figure 1. 2-D OCDMA system using MCM and heterodyne detection.

#### 3.1 MCM Transmitter

At the transmitter, each block of  $m$ -bit is first converted into  $M$  symbols ( $M = 2^m$ ) denoted as  $\{s_u\}$  ( $u = 0, \dots, M - 1$ ) by a converter. Each symbol is then encoded by a corresponding code at a MCM encoder, which can be implemented using fiber Bragg grating (FBG) arrays and an encoding controller as shown in Fig. 2a. The principle of MCM is illustrated in Fig. 2b. The modulated signal, i.e., chip sequence including chip “1s” and “0s”, is then combined to signals from other transmitters and sent to the receiver side over an optical fiber. Note that a chip “1” is corresponding to an optical pulse while a chip “0” means that no pulse is transmitted. In a sequence, the position and wavelength of chip “1s” are determined by symbol’s code.

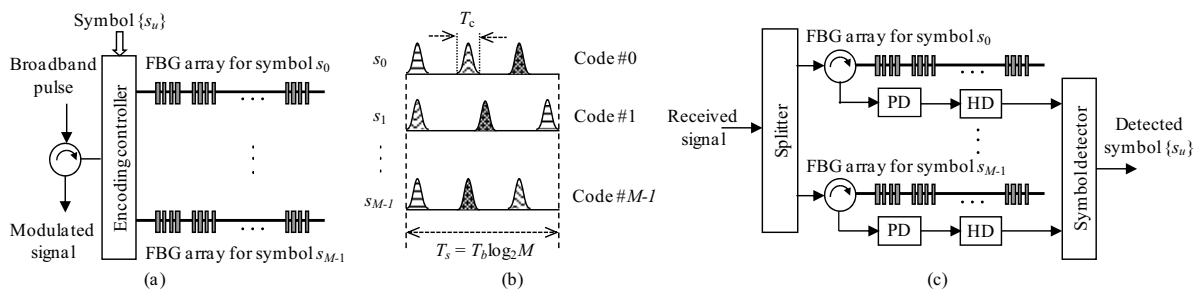


Figure 2. (a) FBG-based MCM encoder, (b) Modulated signal, and (c) FBG-based MCM decoder.

#### 3.2 Linear Dispersive Optical Channel

To analyze impact of GVD, each chip “1” is modeled as a Gaussian optical pulse and optical fiber is considered as a linear dispersive channel. The Gaussian pulse propagation model can be expressed as [6]

$$G(t) = \sqrt{P_0 \exp(-\alpha L)} \frac{T_0}{(T_0^2 - i\beta_2 L)^{1/2}} \exp\left(-\frac{t^2}{2(T_0^2 - i\beta_2 L)}\right), \quad (1)$$

where  $G(t)$  is the amplitude and  $P_0$  is the transmitted peak power of optical pulse.  $T_0$  is half-width of the pulse (at 1/e intensity point).  $\alpha$  and  $\beta_2$  are the attenuation and dispersion coefficients of fiber, respectively.  $L$  is the

fiber length. The received average power per chip can be written as  $P_s = \frac{1}{T_c} \int_{-T_c/2}^{T_c/2} |G(t)|^2 dt$ , where  $T_c$  is the chip duration.

### 3.3 MCM Receiver

At the receiver, the received signal including MAI is first mixed coherently with a local oscillator (LO) whose power per wavelength is  $P_{LO}$ . The LO is a broadband source whose characteristics is the same as the one at the transmitter. The mixed signal is then demodulated at a FBG-based MCM decoder (Fig. 2c). The wavelengths in each FBG array are tuned for the desired symbol's code of the targeted transmitter. Next, the demodulated signal is converted into an electrical signal (at IF signal) by a photodetector (PD). At the PD, OBI will occur due to the beating between chip pulses with nearly the same wavelength. A heterodyne demodulator (HD) is then used to change the IF signal into a baseband one through a synchronous demodulation [6]. In the following step, a symbol detector is used compare its  $M$  inputs in parallel to determine the detected symbol corresponding to the largest value. Finally, the detected symbol is converted into the binary data.

## 4. PERFORMANCE ANALYSIS

In the proposed system, errors happen when the transmitted symbols are wrongly detected. Denote  $P_e$  as the symbol error rate, the BER can be calculated as  $BER = 0.5 MP_e / (M - 1)$  [3]. The following parts will present how to calculate the symbol error rate in two cases mentioned in section 2.2.

### 4.1 Analysis for the case of using multiple code sets

We assume that the probability of that a user transmits any symbol is  $1/M$ . Without loss of generality, we also assume that symbol  $s_0$  is transmitted. Employing a union bound,  $P_e$  can be given as

$$P_e \leq 1 - \Pr\{I_u > I_0 | u \in \{1, \dots, M-1\}, s = s_0\} \leq \sum_{u=1}^{M-1} \Pr\{I_u \geq I_0 | s = s_0\} = (M-1) \Pr\{I_1 \geq I_0 | s = s_0\} \\ = (M-1) \sum_{l_0}^{K-1} \sum_{l_1}^{K-1-l_0} \Pr\{\kappa_0 = l_0, \kappa_1 = l_1\} \Pr\{I_1 \geq I_0 | s = s_0, l_0, l_1\}, \quad (2)$$

where  $I_u$  is the total photocurrent at the  $u$ -th input of the symbol detector,  $s$  represents the transmitted symbol.  $K$  is the number of simultaneous user.  $\kappa_u$  is the random variable that represents the number of interfering users whose transmitted symbol is  $s_u$ , which is a binomial random variable [3]. The probability that  $\kappa_0 = l_0$  and  $\kappa_1 = l_1$ , the first term in equation (2), therefore can be expressed as

$$\Pr\{\kappa_0 = l_0, \kappa_1 = l_1\} = \binom{K-1}{l_0} \left(\frac{1}{M}\right)^{l_0} \left(1 - \frac{1}{M}\right)^{K-1-l_0} \binom{K-1-l_0}{l_1} \left(\frac{1}{M-1}\right)^{l_1} \left(1 - \frac{1}{M-1}\right)^{K-1-l_0-l_1}. \quad (3)$$

At a given input of the symbol detector, a pulse from interfering user becomes an MAI one and reaches this input when it matches one of  $p_s$  FBGs (of corresponding FBG array) in both time delay and wavelength. Denote  $\zeta_u$  as the random variable representing the total number of MAI pulses of the  $u$ -th input,  $\zeta_u$  can be modeled as a binomial random variable with probability  $(\mu_\lambda/p_s^2)$  where  $\mu_\lambda$  is the average number of wavelengths common to a pair of signature codes, which is a function of  $(p_s, p_h^*)$  and can be estimated as [2]. Therefore, the probability that there are  $i_u$  MAI pulses when the total number of interfering users if  $l_u$  can be given as

$$\Pr\{\zeta_u = i_u | l_u\} = \binom{l_u}{i_u} \left(\frac{\mu_\lambda}{p_s^2}\right)^{i_u} \left(1 - \frac{\mu_\lambda}{p_s^2}\right)^{l_u - i_u}. \quad (4)$$

The last term in equation (2) hence can be derived as

$$\Pr\{I_1 \geq I_0 | s = s_0, l_0, l_1\} = \sum_{j=0}^{l_0} \Pr\{\zeta_0 = j | l_0\} \sum_{k=0}^{l_1} \Pr\{\zeta_1 = k | l_1\} Q\left(\frac{I_0 - I_1}{\sqrt{\sigma_0^2 + \sigma_1^2}}\right) \\ = \sum_{j=0}^{l_0} \Pr\{\zeta_0 = j | l_0\} \sum_{k=0}^{l_1} \Pr\{\zeta_1 = k | l_1\} Q\left\{ \frac{\Re \sqrt{2P_{LO}P_s} (p_s + j - k)}{\sqrt{2 \frac{B_e}{B_o} \Re^2 P_s^2 \left(j + \frac{1}{p_s} \binom{j}{2} + \frac{1}{p_s} \binom{k}{2}\right) + \underbrace{2\sigma_{rx}^2}_{\text{Receiver noise}}}} \right\}, \quad (5)$$

where  $Q(x)$  is the  $Q$  function.  $\Re$  is the PD responsivity.  $B_e$  and  $B_o$  are the electrical and optical bandwidth, respectively. The receiver noise includes thermal noise shot noise caused by  $p_s$  LOs [3].

### 4.2 Analysis for the case of using a single code set

Unlike the above case, all symbols in this case belong to the same code set. A pulse from an interfering user can still be a MAI one even when this user transmits different symbol with analyzed one. The first term in equation

(2) is hence removed as  $l_0$  and  $l_1$  are fixed and equal to  $K - 1$ .  $P_e$  in this case is bounded by

$$P_e \leq (M - 1) \Pr\{I_1 \geq I_0 | s = s_0, I_0 = I_1 = K - 1\}. \quad (6)$$

## 5. NUMERICAL RESULTS

We now discuss the numerical results that highlight the advantages of the proposed system over the conventional ones under constraint of average transmitted power per bit ( $P_b$ ). We use bit rate per user  $R_b = 2.5$  Gbps, fiber length  $L = 20$  km, code weight  $p_s = 13$ , and for the sake of fair comparison, we select  $p_h^* = 13$  and  $p_h = 29$  which is the smallest prime number that is larger than  $Mp_h^*$  ( $M = 2$ ).

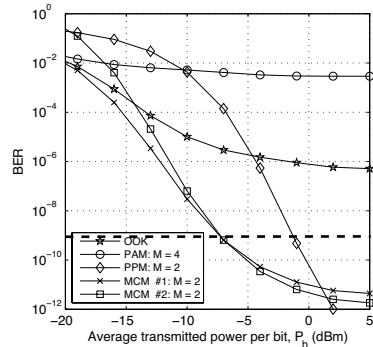


Figure 3. BER vs.  $P_b$  with  $K = 30$ .

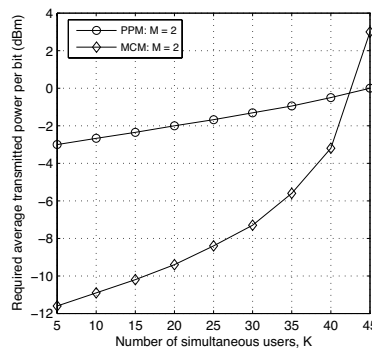


Figure 4. Required power vs.  $K$ .

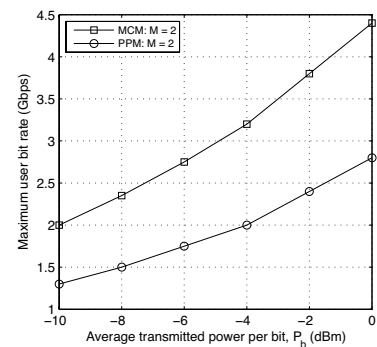


Figure 5.  $R_b$  vs.  $P_b$  with  $K = 30$ .

In Fig. 3, we compare the performance of the proposed system with the ones using OOK, 4-level PAM, and 2-level PPM when  $K = 30$  users. BER floors in the figure are determined by MAI since OBI is relaxed by heterodyne detection. The result shows that PAM system is most affected by MAI hence has worst performance (highest BER floor). Similarly, MAI is dominant in OOK system and its BER floor cannot reach  $10^{-9}$ . The PPM system has lowest BER floor thanks to its ability of reducing MAI. However, the required transmitted power in PPM system is relatively high (above 0 dBm) due to the impact of GVD. In the power range of  $P_b \leq 0$  dBm, which is preferable for access networks, the proposed system allows for both lower BER and smaller required power than any other systems.

Figure 3 also shows that, the difference in performance of the system using a single code set (MCM #1) and multiple code sets (MCM #2) is not much. However, using single code set has an advantage that, with the fixed number of wavelengths ( $p_h$ ), we can apply higher level of modulation ( $M$ ) to get the better performance, whereas, for the case of using multiple code sets,  $M$  is limited since  $p_s \leq p_h^*$  and  $Mp_h^* \approx p_h$ .

The required transmitted power per bit, when  $\text{BER} = 10^{-9}$ , of the PPM system and proposed system are compared in detail versus the number of simultaneous users in Fig. 4. When  $K < 42$  users, the required power of the proposed system is lower than that of PPM system. The reason is that the impact of GVD in this case is stronger than MAI. When  $K \geq 42$  users, MAI is dominant and PPM system requires lower transmitted power.

Finally, the maximum user's bit rate versus the transmitted power is shown in Fig. 5 when  $K = 30$  users. At the same transmitted power, the proposed system can support higher bit rate than PPM one. For example, at  $P_b = -2$  dBm, the maximum bit rate per user is 3.8 Gbps in the proposed system, whereas it is 2.5 Gbps in PPM system.

## 6. CONCLUSIONS

We have proposed a new modulation scheme of MCM for 2-D OCDMA systems. The combination of MCM and heterodyne detection helps to simultaneously reduce the impact of MAI, OBI, and GVD, which allows for lower BER, lower required power, and higher user's bit rate than the 2-D OCDMA systems using conventional modulation schemes. The advantages obtained from the proposed system are crucial for the feasibility of 2-D OCDMA in the next generation broadband access networks.

## REFERENCES

- [1] L. Tancevski, I. Andonovic: Hybrid wavelength hopping/time spreading schemes for use in massive optical networks with increased security, *IEEE J. Lightwave Technol.*, vol. 14, no. 12, pp. 2636-2647, Dec. 1996.
- [2] L. Tancevski, L. A. Rush: Impact of the beat noise on the performance of 2-D optical CDMA systems, *IEEE Commun. Lett.*, vol. 4, no. 8, pp. 264-266, Aug. 2000.
- [3] A. T. Pham, H. Yashima: Performance enhancement of 2-D WH/TS OCDM systems using a heterodyne detection receiver and PPM signaling, *OSA J. Optical Networking*, vol. 6, no. 6, pp. 789-800, Jun. 2007.
- [4] T. Miyazawa, I. Sasase: Enhancement of tolerance to MAIs by the synergistic effect between M-ary PAM and the chip-level receiver for optical CDMA systems, *IEEE J. Lightwave Technol.*, vol. 24, no. 2, pp. 658-666, Feb. 2006.
- [5] N. T. Dang *et al.*: Impact of GVD on the performance of 2-D WH/TS OCDMA systems using heterodyne detection receiver, *IEICE Trans. on Fundamentals*, vol. E92-A, no. 4, pp. 1182-1191, Apr. 2009.
- [6] G. P. Agrawal: *Fiber-Optic Communication Systems*, A John Wiley and Sons, 2002.